

Mitigation of the Ionospheric Range Error in Single-frequency GNSS Applications

C. Mayer, N. Jakowski, J. Beckheinrich, and E. Engler
*Institute of Communications and Navigation, German Aerospace Center
Kalkhorstweg 53, 17235 Neustrelitz, Germany*

BIOGRAPHY

Christoph Mayer is a research scientist at the German Aerospace Center. He received his PhD from the University of Jena in 2005. Having a background in theoretical physics, his current work involves monitoring and modeling the ionosphere for GNSS applications.

Norbert Jakowski, is holding a PhD from the University of Rostock. Since 1974 he has been working in the Institute of Space Research, since 1991 in the German Aerospace Center in Neustrelitz. He is experienced in monitoring and modeling the ionosphere based on trans-ionospheric radio sounding methods.

Jamila Beckheinrich received her Diploma in Geodesy from the University of Berlin in 2006. Her principal area of research and work is the development and implementation of RTK algorithms

Evelin Engler is holding a PhD from the Technical University of Dresden. She is involved in the project management of GBAS related projects and her principal area of research and work is the development of GNSS signal monitoring algorithms.

ABSTRACT

We describe a method which allows to autonomously determine the ionospheric range error using single-frequency GNSS data of a single GNSS receiver. The proposed algorithm is capable of deriving calibrated ionospheric range errors from single-frequency GNSS data. In addition, a model describing the ionosphere in the vicinity of the receiver is provided, along with various statistical quantities. In the context of single-frequency point positioning, e.g., using low-cost GNSS receivers in quasi-static setups, this method is anticipated to provide autonomously determined, near-real-time ionospheric corrections comparable or better than the Klobuchar model. In (civil) aeronautical GBAS systems, which due to certification issues will continue to be restricted to use single-frequency GNSS equipment for some time, this

method allows to detect ionospheric perturbations, including ionospheric gradient information.

INTRODUCTION

A significant number of GNSS applications uses single-frequency GNSS receivers. Therefore the precise estimation of the ionospheric range error from single-frequency GNSS data is and remains to be an important issue.

One option to correct the ionospheric range error in single-frequency applications is the use of models such as the Klobuchar model for GPS [1,2,4] or the NeQuick model [3] foreseen for use in GALILEO, the planned European GNSS. Another option is to use correction data provided by an additional augmentation service such as the Wide Area Augmentation Systems (WAAS) in the US or the European Geostationary Overlay Service (EGNOS) in Europe. Finally, there is the option to derive the ionospheric correction term from code and carrier phases provided by single-frequency receivers which we consider in this paper.

ESTIMATION OF IONOSPHERIC RANGE ERROR

In order to estimate the ionospheric range error, the raw GPS data has to be pre-processed. This includes code-phase smoothing, removal of outliers and cycle slips and Geo-referencing, *i.e.*, calculation of elevation and azimuth of the data samples. This processing scheme is common standard in related work to estimate the total electron content (TEC) of the ionosphere, *cf.* [5] and references therein.

In a good approximation the ionospheric range error is related to the total electron content by

$$I = \frac{40.3}{f^2} \cdot TEC \quad (1)$$

with

I ionospheric range error at frequency f [m]
where TEC is the number of electrons per unit area along the path of propagation, *i.e.*

$$TEC = \int n_e ds \quad (2)$$

with

n_e electron density.

While the standard methods for deriving TEC rely on *dual*-frequency GPS data, *cf.* [5], here we outline a method to derive TEC from *single*-frequency data. This concept becomes more and more attractive as pseudo-range noise is reduced in modern receivers.

The method is based on the fact that the ionospheric plasma affects the phase and pseudo-range measurements with opposite signs [6]. This is due to the different phase and group velocities of electromagnetic waves in the ionospheric plasma. Therefore, we can compute the *relative* ionospheric range error by taking the difference between code and phase measurements:

$$\psi_n - \varphi_n = 2 \cdot I_n + \varepsilon_n + b_n \quad (3)$$

with

ψ_n phase measurement at epoch n [m]

φ_n pseudo-range measurement at epoch n [m]

where we have denoted all noises as ε , and collectively denoted all instrumentation offsets and the phase ambiguities as b .

In order to suppress the dominant noise contribution, the code multi-path noise, we use a simple low-pass filter with a suitably chosen time constant τ , *i.e.*, the smoothed code-phase difference y_n at time t is formed by averaging $(\rho - \varphi)$ in the time interval $(t - \tau/2, t + \tau/2]$. In addition to noise suppression, this data smoothing provides error covariances σ_I which are adapted to the data. Another way of obtaining σ_I would be to use a fixed, elevation-dependent model; however such a model has to be manually adapted to different types of data. The smoothing time constant τ has to be adapted to the input data for the algorithm. Here we use a time constant $\tau \approx 5$ min.

For the smoothed code-phase differences, $y = \psi - \varphi$, the measurement model (3) becomes

$$y = 2 \cdot I + b \quad (4)$$

Note that there is a specific phase ambiguity for each data arc, *i.e.*, a continuous range of receiver-satellite measurements. Thus, we have to determine a new constant b for each new data arc in order to calibrate the relative ionospheric range errors obtained from the filtered difference of phase and code observables.

The following plot shows relative TEC data determined from single frequency GPS measurements sampled with 1 Hz of the station KRUM (Germany), along with the smoothed relative TEC values and errors derived in the process of smoothing.

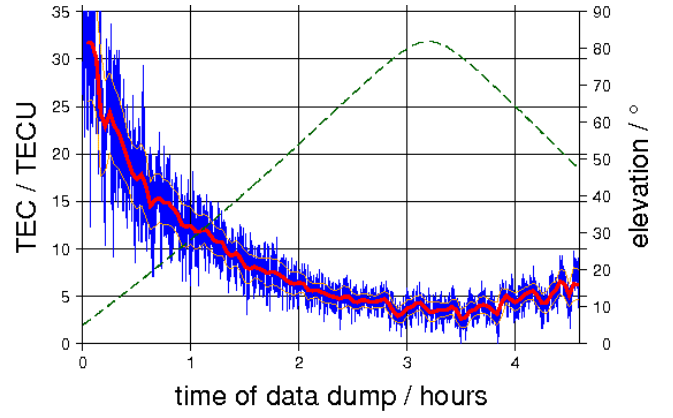


Fig 1

The relative ionospheric range error computed from the difference of code and phase measurements is shown (blue), along with the elevation (green) and the smoothed relative range error (red). $1 \text{ TECU} = 10^{16} \text{ m}^{-2}$

LOCAL IONOSPHERE MODEL

Our local ionosphere model approximates the altitude-dependent electron density distribution by a single layer at height 400 km. The spatial and temporal variations of the vertical ionospheric delay I_V near the receiver are parameterized by a (linear) polynomial,

$$I_V(u_1, u_2) = a_0 + a_1 \cdot u_1 + a_2 \cdot u_2 \quad (5)$$

using three coefficients a_0 , a_1 , and a_2 . The coordinates (u_1, u_2) refer to a local sun-fixed coordinate system, centered at the receiver position. Given latitude, longitude, and time differences Δlat , Δlon , and ΔT between the ionospheric pierce point and the reference receiver, the coordinates (u_1, u_2) are given by

$$\begin{pmatrix} u_1 \\ u_2 \end{pmatrix} = \begin{pmatrix} \Delta \text{lon} + \Delta T \cdot 15^\circ \\ \Delta \text{lat} \end{pmatrix} \quad (6)$$

The *slant* ionospheric delay is related to the vertical ionospheric delay by an elevation-dependent mapping function G ,

$$I(\text{elev}, u_1, u_2) = G(\text{elev}) \cdot I_V(u_1, u_2) \quad (7)$$

which is defined as

$$G(\text{elev}) = \left(1 - \left(\frac{r_E \cos(\text{elev})}{r_E + h_{\text{Iono}}} \right)^2 \right)^{-1/2} \quad (8)$$

where

r_E Earth's radius: 6371 km

h_{Iono} height of single layer ionosphere: 400 km

elev Satellite elevation [rad]

The model (5) describes the ionosphere around the reference station as a plane w.r.t. the sun-fixed coordinates used here; the coefficient a_0 parameterizes the

absolute value of ionization over the reference station, while the coefficients a_1 and a_2 contain ionospheric gradient information. Note that these gradients are large-scale gradients. Small-scale ($\approx 50\text{km}$) gradients cannot be modelled by this simple linear model. However, in the reconstruction technique described in the next Section there is a statistical parameter which indicates if the model is not consistent with the data. It is possible to use generalize the model in (5) by using higher order polynomials in (u_1, u_2) .

ESTIMATION OF IONOSPHERE MODEL

Given the smoothed code-phase difference measurements y with errors σ_i , we estimate the state vector x , which consists of model parameters a_0, a_1, a_2 and offsets b , in two phases:

- least squares minimization at start-up determines an initial solution
- recursive filtering after an initial solution has been found

During the start-up phase we determine an initial solution for the parameters x by minimizing the cost function

$$S_0(x) = \frac{1}{2}(y - Ax)^T C_0^{-1}(y - Ax) \quad (9)$$

with $C_0 = \text{diag}(\sigma_i^2)$, where the matrix A is determined the model, *cf.* Eq. (4), and C_0 is given by the pre-processing. After the initial model parameters have been determined, we use a form of recursive filtering with cost function

$$S_1 = S_0 + \frac{1}{2}(P^T x - x')^T C^{-1}(P^T x - x') \quad (10)$$

Here, x' and C' denote the model parameters and covariance from the previous time step propagated to the current time step,

$$x_n' = T x_{n-1} \quad (11)$$

$$C_n' = T^T C_{n-1} T + C_m$$

and P is a projector from the previous epoch to the current epoch. The model covariance, C_m , encodes the uncertainty of the time update. For the model (5) the time propagation matrix T is

$$\begin{pmatrix} \mathbf{1} & dt \cdot \mathbf{15}^\circ & \mathbf{0} \\ \mathbf{0} & \mathbf{1} & \mathbf{0} \\ \mathbf{0} & \mathbf{0} & \mathbf{1} \end{pmatrix} \quad (12)$$

where the off-diagonal entry originates from the local-time dependence of the u_1 coordinate, *cf.* Eq. (6).

The second summand in Eq. (10) demands that the state vector x (*i.e.* the model coefficients a_0, a_1, a_2 and the offsets b) does not change between adjacent epochs; this is reasonable, since the offsets b are supposed to be constant and the model coefficients are to first order constant, too, since we use sun-fixed coordinates. Note

that the projector P is needed since in the current epoch there may not be all observations of the previous epoch present.

We have applied the single-frequency single-station ionosphere estimation technique outlined above to different types of data from GPS receivers situated at high- mid- and low-latitude positions. For the start-up phase we used data collected during 4 hours around local midnight; the recursive filtering steps were performed every 10 minutes.

- In Fig. 2 we have plotted the vertical ionospheric delay over Neustrelitz (Germany) obtained from single-frequency GPS data collected in July 2006 with TEC data from SWACI [8]. The daily variation of TEC is clearly visible. Both curves agree quite well. This comparison is encouraging, taking into account that we compare TEC values determined from a single station using single-frequency GNSS data with TEC maps which are produced using dual-frequency phase and code GNSS data from a network of 20-30 GNSS receivers.
- Fig. 3 shows TEC reconstructed from single-frequency GPS data in Bandung (Indonesia). Compared to Neustrelitz, TEC levels are much higher, as well as the gradient coefficients. The plateau after local sunset (12-15 UTC) is most likely due to the collapsing ionosphere compensated by the enhanced fountain effect.

In both data samples the relative χ^2 value of the reconstructions (which is just S_1 evaluated at the solution divided by the number of degrees of freedom) is below 1, indicating that the model (5) is consistent with the data, given the data and model covariance matrices C_0 and C_m .

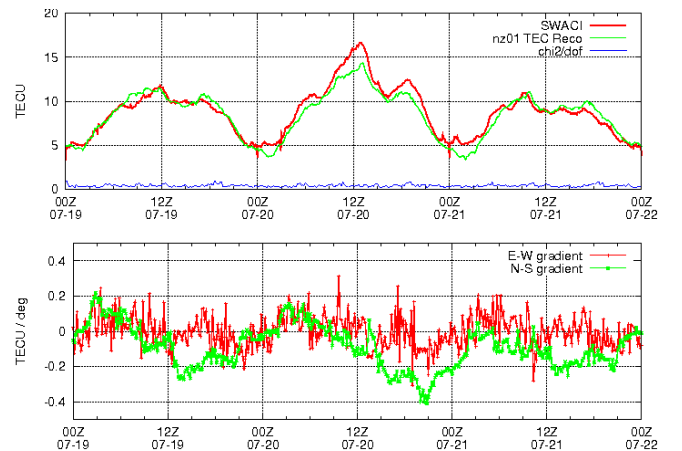


Fig 2: Top: comparison of vertical TEC at $53^\circ 20'E$, $13^\circ 04'N$ (Neustrelitz, Germany) Jul 19-22 2006 between single-station derived TEC (in green) and SWACI TEC values (red). The blue curve shows the relative χ^2 value of the fit. Bottom: ionospheric gradients, *i.e.*, the coefficients a_1 and a_2 derived from the recursive filter (1 TECU/deg ≈ 1.44 mm/km).

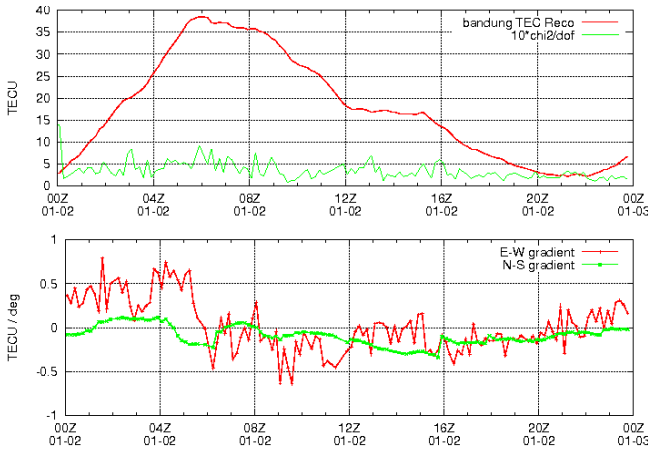


Fig 3: Vertical TEC and TEC gradients at 6°54'S, 107°35'E (Bandung, Indonesia) Jan 2 2006.

POSITION SOLUTION

In this Section we investigate to which degree the estimated ionospheric delays of the last Section can improve a single-point single-frequency position solution using carrier-smoothed input data. The position solution algorithm consists of the chain of processing shown in Fig. 4: before calculating the user position, cycle slip detection is performed, followed by single carrier smoothing. The processor is also extended by a Detection, Identification and Application (DIA) algorithm, *cf.* [9,10], in order to control and remove outliers from the observation data.

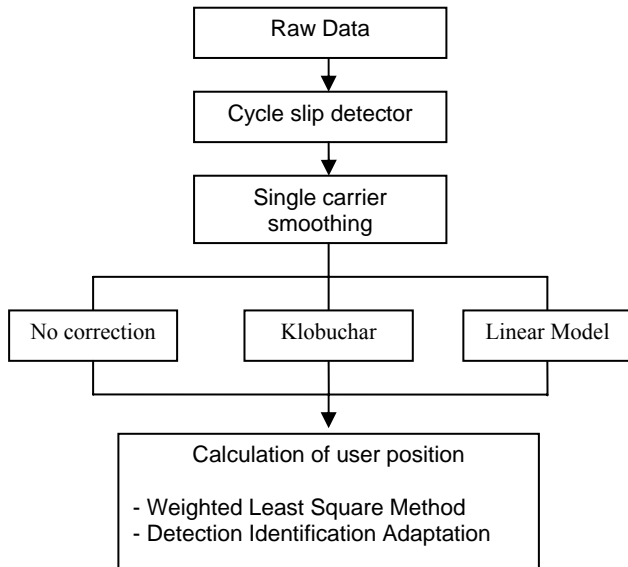


Fig 4: Chain of processing for position solution

The calculation of the user's position is based on the least-squares method. While the stochastic model used in this first prototype is a simplified unit matrix, in the future it is foreseen to use weighting coefficients obtained from the real-time estimation of signal performance quantities.

In the case of single frequency navigation processing considered here, a smoothed range s_n can be determined by calibrating the ambiguous phase with the low-pass filtered difference of code and carrier measurements (Hatch filter [7]):

$$\begin{aligned} \chi_n &= \psi_n - \varphi_n \\ \overline{\chi_n} &= \left(\mathbf{1} - \frac{\mathbf{1}}{T} \right) \overline{\chi_{n-1}} + \frac{\mathbf{1}}{T} \cdot \chi_n \\ s_n &= \varphi_n + \overline{\chi_n} \\ s_n &= \varphi_n + \frac{\mathbf{1}}{T} \sum_{k=0}^n \left(\mathbf{1} - \frac{\mathbf{1}}{T} \right)^{n-k} \cdot (\psi_k - \varphi_k) \end{aligned} \quad (13)$$

The accuracy of such derived smoothed ranges is influenced by three different effects:

- At begin of the low-pass filtering a transient effect can be observed at the filter output, which corresponds with the crossover between the initial difference of range and phase measurements and its weighted average after a suitable long filtering time. If the filtering time is in the order of the fourfold time constant of the filter, the residual error is cut down on 1% of crossover's magnitude (*cf.* Fig. 5).

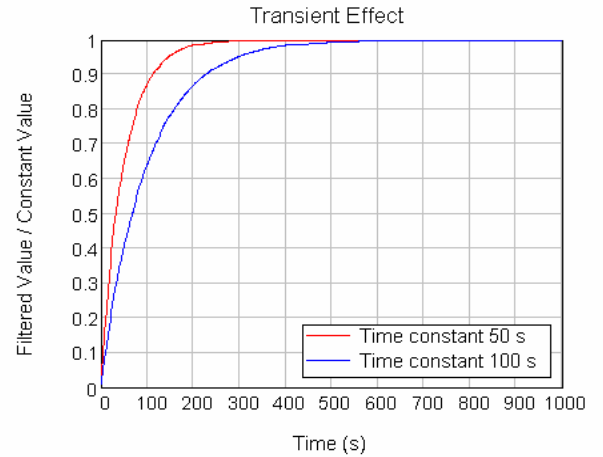


Fig 5: Ratio of filtered and unfiltered constant value in dependence on the used time constant

- Multipath and coloured noise are temporal correlated processes with changing characteristics during a satellite path. If the standard deviation of temporal correlated noise and multipath shall be reduced on the half (Fig. 6), the selected time constant should be fulfilled following condition involving the autocorrelation function (*acf*) of the noise:

$$\frac{akf(T)}{akf(0)} \approx 0.1 \quad (14)$$

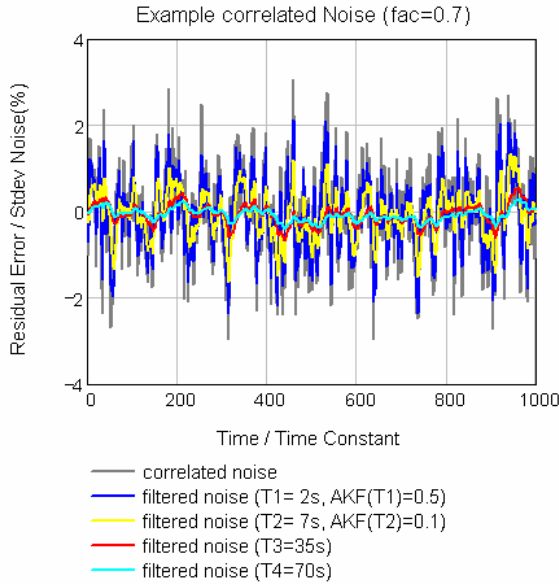


Fig 6: Noise reduction for different time constants in relation to the autocorrelation of the noise

- Due to the opposite sign of the ionospheric propagation error in the range and phase measurements the difference of both includes a drifting part. Induced by the reaction time of the filter process, the output lags to the momentary ionospheric propagation error. The magnitude of this lag effect depends on the drift itself and the used time constant of the filter (Fig. 7).

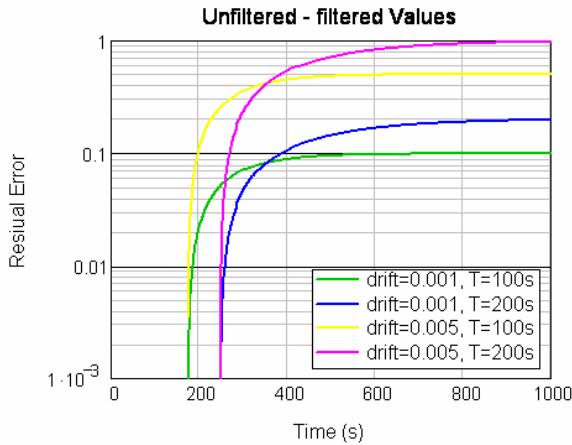


Fig 7: Residual error at the filter output respectively a drifting input induced by the reaction time of the filter

Consequently, it must be assumed that the smoothed ranges used for ionospheric modelling own different accuracies. A common valid optimised time constant of the filter can not be determined due to opposite

requirements (large for a good multipath reduction, small for a short transient effect and a reduced lag error) and due to the temporal variation of the propagation effects.

RESULTS

In order to demonstrate the performance of the different ionospheric models a representative example is discussed in the following, using GPS raw data sampled with 50Hz obtained from Tromsø (Norway) on Nov 7 2003. The high sampling frequency is necessary for the cycle-slip detection algorithm; the position solution was computed every 30 seconds.

Table 1 shows the mean offset to the reference position, using no ionospheric correction, Klobuchar model ionospheric correction, and the proposed ionospheric correction described here. In the used time period of 24 hours, the 3D error is smallest when using the linear model (5). Similarly the height deviation is smallest when using the linear model.

Table 1: Mean offset to reference position.

Used Model	3D/m	Δ lon/m	Δ lat/m	Δ h/m
No Correction	4.208	0.532	0.009	3.585
Klobuchar	2.993	0.256	0.147	-1.380
Linear Model	2.720	0.516	-0.012	0.800

2875 Epochs. Nov 7 2003, Tromsø: 69°40'N, 18°56'E

Table 2 shows the RMS of the differences to the reference position. Here, the linear model corrections perform as good or better as the Klobuchar model corrections. Again the improvement is most pronounced in the height resolution.

Table 2: RMS of difference to reference position

Used Model	3D/m	Δ lon/m	Δ lat/m	Δ h/m
No Correction	4.768	1.274	1.230	4.427
Klobuchar	3.346	1.071	1.156	2.952
Linear Model	3.137	0.953	1.212	2.732

2875 Epochs. Nov 7 2003, Tromsø: 69°40'N, 18°56'E

The improvement of the ionospheric corrections of the model (5) compared to Klobuchar model corrections is noticeable but relatively small. Note, however, that there is a significant improvement in the height direction, which is important for GNSS aviation applications. Further work is planned, such as analysing more than one day of data, and using a more realistic error model as input for the position solution.

CONCLUSIONS

We have developed a model-assisted TEC calibration and reconstruction technique, using a single-layer model of the ionosphere valid in the vicinity of the GNSS receiver.

This technique is capable of calibrating the relative ionospheric range errors in near-realtime by using a form of recursive filtering based on weighted least-squares minimization (9-12); the input measurement errors are determined from the Hatch-type filtering, while the initial model covariances may be determined by the start-up weighted-least-squares solution.

Along with the model coefficients describing the variation of vertical TEC around the receiver we obtain further statistical information, e.g., the relative χ^2 value of the fit which is a measure of how good the model Ansatz is consistent with the measured data, given the measurement errors and model covariances.

We have applied the algorithm to the reconstruction of vertical TEC from dual-frequency phase-only GNSS data. Here, the relative χ^2 values are quite high, signalling that the simple single-layer polynomial ionospheric model cannot fully describe the ionospheric information contained in the low-(multipath-)noise GNSS phase observables. Nevertheless, calibrated TEC can be obtained with this method from phase-only GNSS data. A possible continuation along the lines of this route would be to consider more elaborated ionospheric models, possibly transcending the single-layer approximation.

The comparison of vertical TEC derived from single-station single-frequency data obtained by the proposed method with TEC values obtained from European TEC maps under near-solar-minimum conditions shows a good agreement. These European TEC maps are routinely provided by the ionospheric data service SWACI [8]. The proposed algorithm has been tested under different geophysical conditions, e.g., at different latitudes, seasons, and levels of solar activity.

Besides comparing the ionospheric range error with other ionospheric data and models, we have compared the performance of our corrections in single-frequency point positioning with Klobuchar-model-derived ionospheric corrections and shown that our corrections perform as good or better than the Klobuchar model corrections.

ACKNOWLEDGMENTS

CM and NJ gratefully acknowledge support of the German state government of Mecklenburg-Vorpommern under the grant number AU-07008 (SWACI).

REFERENCES

[1] Enge, P. and Misra P., Global Positioning System - Signals, Measurements, and Performance, Ganga-Jamuna Press, 2nd edition, 2006.

- [2] GPS Interface Control Document 200C
<http://www.navcen.uscg.gov/pubs/gps/icd200/>
- [3] Hochegger, G., B. Nava, S.M. Radicella and R. Leitinger (2000): A family of ionospheric models for different uses, *Phys. Chem. Earth*, 25 (4), 307-310.
- [4] Klobuchar, J., Ionospheric time-delay algorithm for single frequency GPS users, *IEEE Trans. Aerospace and Electronic Systems*, 23, 325-332, 1987
- [5] Jakowski, N., TEC Monitoring by Using Satellite Positioning Systems, in *Modern Ionospheric Science*, (Eds. H. Kohl, R. Rüster, K. Schlegel), EGS, Katlenburg-Lindau, ProduServ GmbH Verlagsservice, Berlin, pp 371-390,1996
- [6] Blewitt, G., 1990. An automatic editing algorithm for GPS data. *Geophys. Res. Lett.* 17, pp. 199-202.
- [7] Hatch, Ronald R. and Knight, Jerry E., Method and apparatus for smoothing code measurements in a global positioning system receiver, United States Patent 5471217
- [8] SWACI: Space Weather Application Center Ionosphere, <http://w3swaci.dlr.de>
- [9] Xin-Xiang Jin, A recursive Procedure for Computation and Quality Control of GPS Differential Corrections, LGR-Series Publications of the Delft Geodetic Computing Center No. 8, April 1995
- [10] Teunissen P.J.G., Quality Control in Geodetic Networks, Delft University of Technology, Reports of the Department of geodesy, 1984EVNet TODO